Space Instrumentation (3)

Lectures for the IMPRS June 23 to June 27 at MPAe Lindau
Compiled/organized by Rainer Schwenn, MPAe,
supported by Drs. Curdt, Gandorfer, Hilchenbach, Hoekzema, Richter, Schühle

Mon, 23.6., 16:00 Plasma detectors. Electrostatic analyzers: From particle counting to moments of distribution function. Helios, Giotto IMS, TAUS (RS)

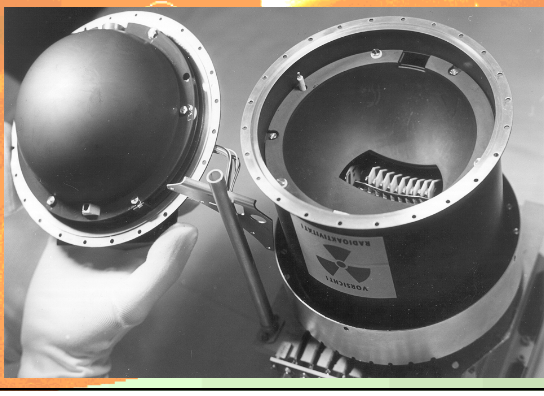

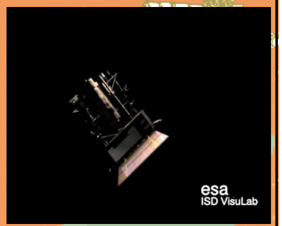

The principle of electrostatic analyzers

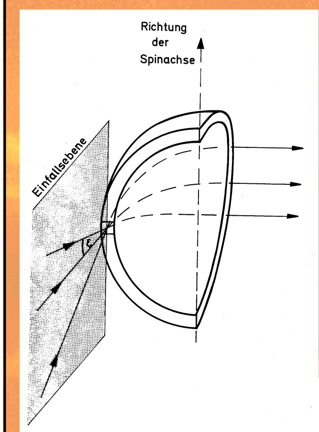

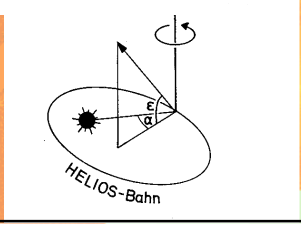

- Spherical deflection plates (radius R, plate distance d) with an applied voltage (U) let charged particles (mass m, ion charge q, velocity v) pass if their energy/charge (E/q) fits, i.e., if
  $$E/q\ (= m/2 * V^2/q) = UR/2d.$$
- Detectors at the exit of the plates count the successful particles.
- Quadrispheric plates with several detectors allow determination of one angle of incidence.
- Rotation of the detector, e.g., on a spinning spacecraft, allows determination of the other angle of incidence.
- The voltage is stepped through and the successful particles per step are counted.
- This way, the particle fluxes of all energy/charge values at all angles of incidence can be measured and a 3D velocity distribution function can be derived.

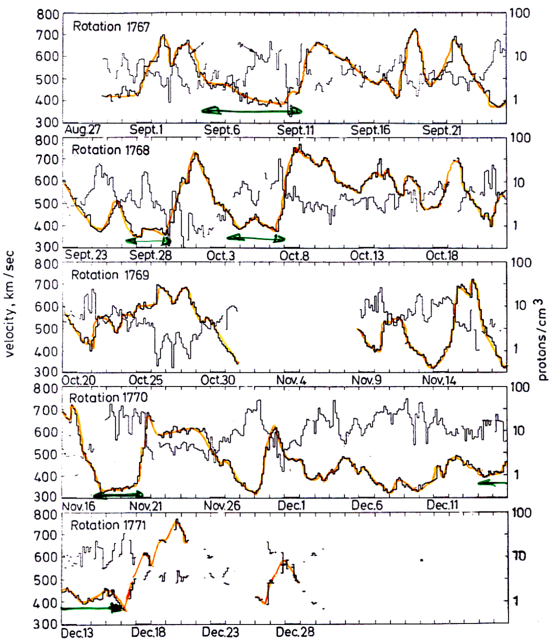

Fig. 1.5 Three-hour averages of the solar wind proton density and flow speed observed by Mariner 2 in 1962 [1.21]. The time coordinate has been broken into 27-day solar rotation periods

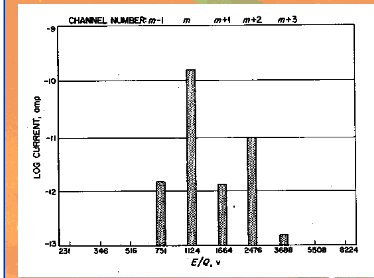

One of the first E/Q spectra, proving the existence of the solar wind

Gringauz (1960) and finally Neugebauer and Snyder (1962) observed the solar wind, using very simple plasma detectors on board interplanetary spacecraft

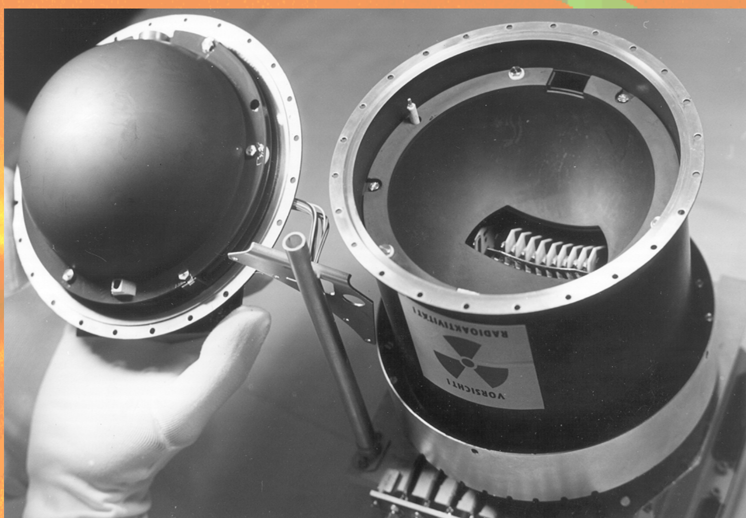

The ion instruments on Helios 1&2, built at MPE Garching (H. Rosenbauer, PI).
Left: a hemispherical analyzer, using an elctrometer for counting charges.
Right: a quadrispherical analyzer for counting particles.

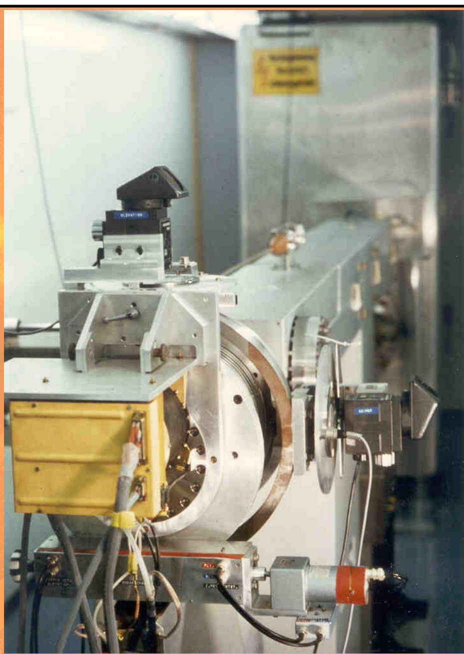

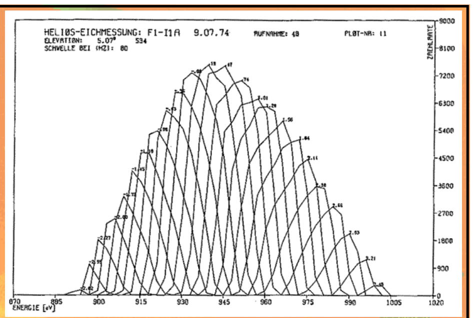

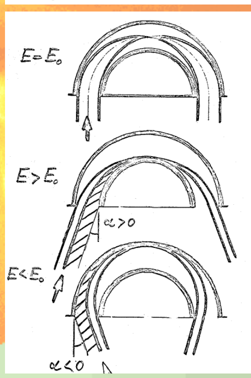

The energy-angle dependence requires careful calibrations!

The calibration facilitiy at MPE and MPAe

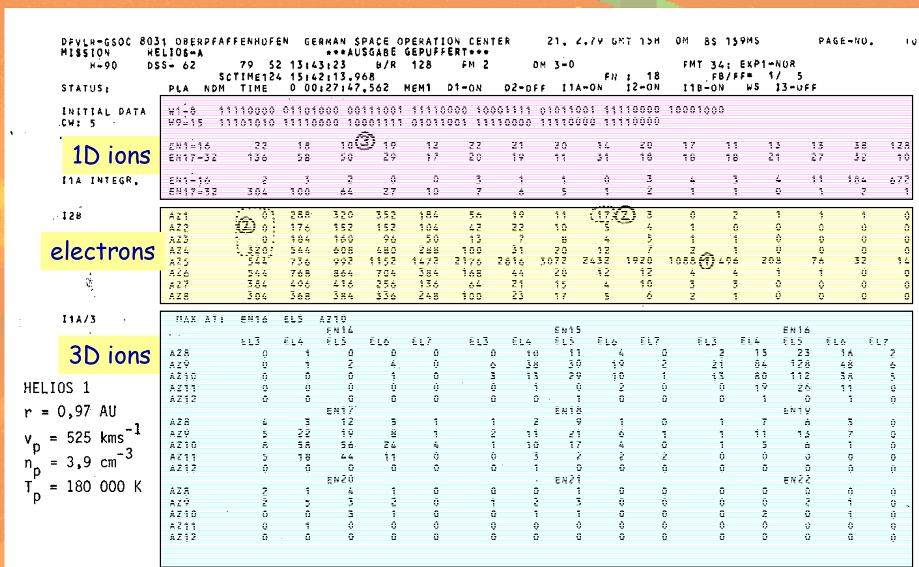

DFVLR-GSOC 8031 OBERPFAFFENHOFEN GERMAN SPACE OPERATION CENTER 21. 2.79 GMT 15H 0M 8S 159MS PAGE-NO.
MISSION HELIOS-A ***AUSGABE GEPUFFERT***
H-90 DSS- 62 79 52 13:43:23 B/R 128 FM 2 OM 3-0 FMT 34: EXP1-NOR
SCTIME124 15:42:13.968 FN : 18 FB/FF= 1/ 5
STATUS: PLA NDM TIME 0 00:27:47.562 MEM1 D1-ON D2-OFF I1A-ON I2-ON I1B-ON WS I3-OFF

INITIAL DATA
CW: 5
W1-8 11110000 01101000 00111001 11110000 10001111 01011001 11110000 10001000
W9-15 11101010 11110000 10001111 01011001 11110000 11110000 11110000

1D ions

EN1-16	22	18	10	19	12	22	21	20	14	20	17	11	13	13	38	128
EN17-32	136	58	50	29	17	20	19	11	31	18	18	18	21	27	32	10

I1A INTEGR.

EN1-16	2	3	2	0	0	3	1	1	0	3	4	3	4	11	184	672
EN17-32	304	100	64	27	10	7	6	5	1	2	1	1	0	1	2	1

I2B

electrons

AZ1	0	288	320	352	184	56	19	11	17	3	0	2	1	1	1	0
AZ2	0	176	152	152	104	42	22	10	5	4	1	0	0	0	0	0
AZ3	0	184	160	96	50	13	7	8	4	5	1	1	0	0	0	0
AZ4	320	544	608	480	288	100	31	20	12	7	2	1	0	0	0	0
AZ5	544	736	992	1152	1472	2176	2816	3072	2432	1920	1088	496	208	76	32	14
AZ6	544	768	864	704	384	168	44	20	12	12	4	4	1	1	0	0
AZ7	384	496	416	256	136	64	21	15	4	10	3	3	0	0	0	0
AZ8	304	368	384	336	248	100	23	17	5	6	2	1	0	0	0	0

I1A/3

3D ions

MAX AT: EN16 EL5 AZ10

	EN14					EN15					EN16				
	EL3	EL4	EL5	EL6	EL7	EL3	EL4	EL5	EL6	EL7	EL3	EL4	EL5	EL6	EL7
AZ8	0	1	0	0	0	0	10	11	4	0	2	15	23	16	2
AZ9	0	1	2	4	0	6	38	30	19	2	21	84	128	48	6
AZ10	0	0	0	1	0	3	13	29	10	1	13	80	112	38	5
AZ11	0	0	0	0	0	0	1	0	2	0	0	19	26	11	0
AZ12	0	0	0	0	0	0	0	1	0	0	0	1	0	1	0
	EN17					EN18					EN19				
AZ8	4	3	12	5	1	1	2	9	1	0	1	7	6	3	0
AZ9	5	22	19	8	1	2	11	21	6	1	1	11	13	7	0
AZ10	8	58	56	24	4	1	10	17	4	0	1	5	6	1	0
AZ11	5	18	44	11	0	0	3	2	2	2	0	0	0	0	0
AZ12	0	0	0	0	0	0	1	0	0	0	0	0	0	0	0
	EN20					EN21					EN22				
AZ8	2	1	4	1	0	0	0	1	0	0	0	0	0	0	0
AZ9	2	5	3	2	0	1	2	3	0	0	0	0	2	1	0
AZ10	0	0	3	1	0	0	1	1	0	0	0	2	0	1	0
AZ11	0	1	0	0	0	0	0	0	0	0	0	0	0	0	0
AZ12	0	0	0	0	0	0	0	0	0	0	0	0	0	0	0

HELIOS 1
r = 0,97 AU
v_p = 525 kms^{-1}
n_p = 3,9 cm^{-3}
T_p = 180 000 K

A printout of Helios-E1 raw data

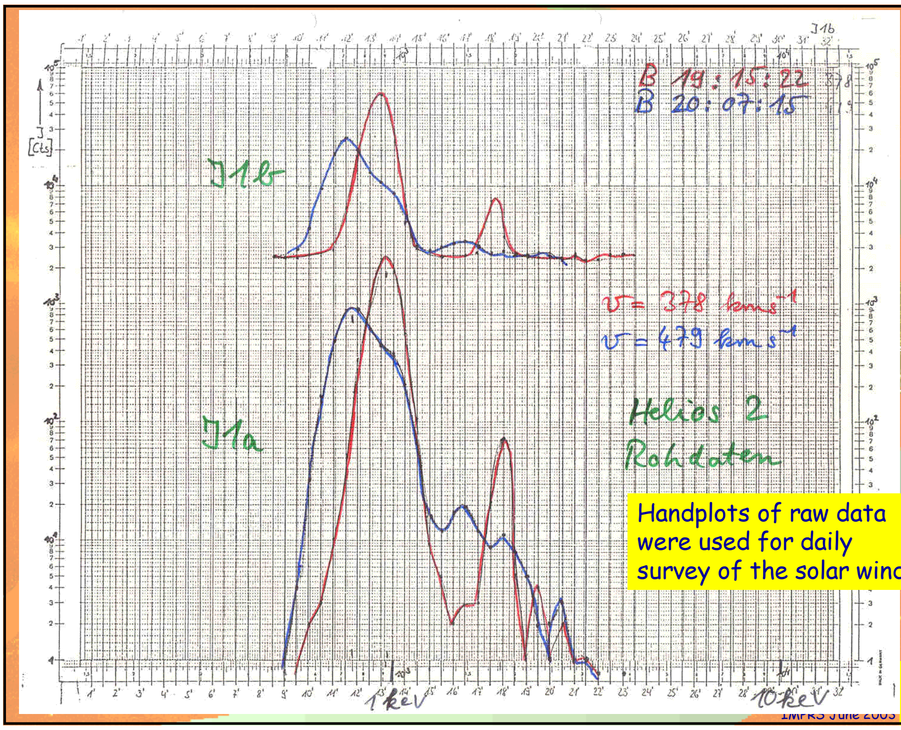

Handplots of raw data were used for daily survey of the solar wind

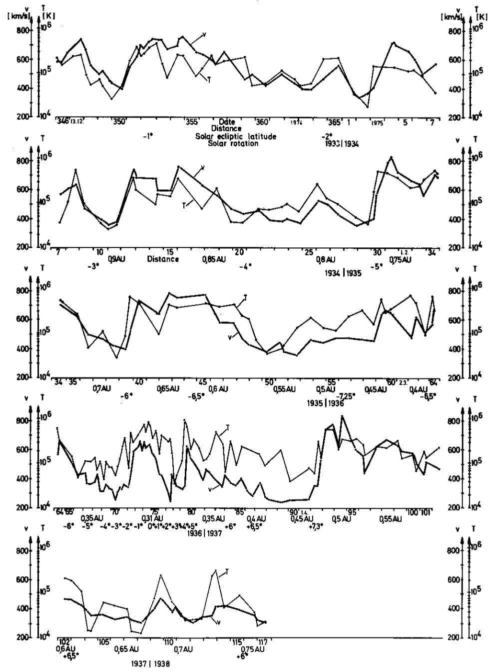

Solar wind basic properties from daily handplots for the first few solar rotations during appoach of Helios 1 to perihelion.

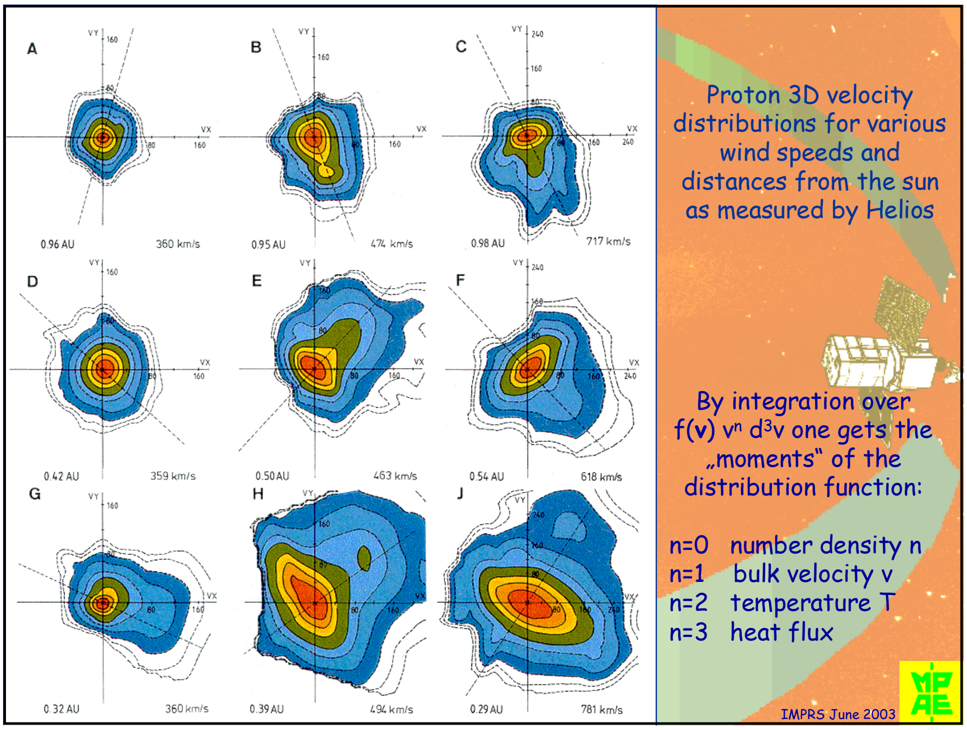
A
B
C
D
E
F
G
H
J
0.96 AU
360 km/s
0.95 AU
474 km/s
0.98 AU
717 km/s
0.42 AU
359 km/s
0.50 AU
463 km/s
0.54 AU
618 km/s
0.32 AU
360 km/s
0.39 AU
494 km/s
0.29 AU
781 km/s
Proton 3D velocity distributions for various wind speeds and distances from the sun as measured by Helios
By integration over f(v) vⁿ d³v one gets the „moments" of the distribution function:
n=0 number density n
n=1 bulk velocity v
n=2 temperature T
n=3 heat flux
IMPRS June 2003

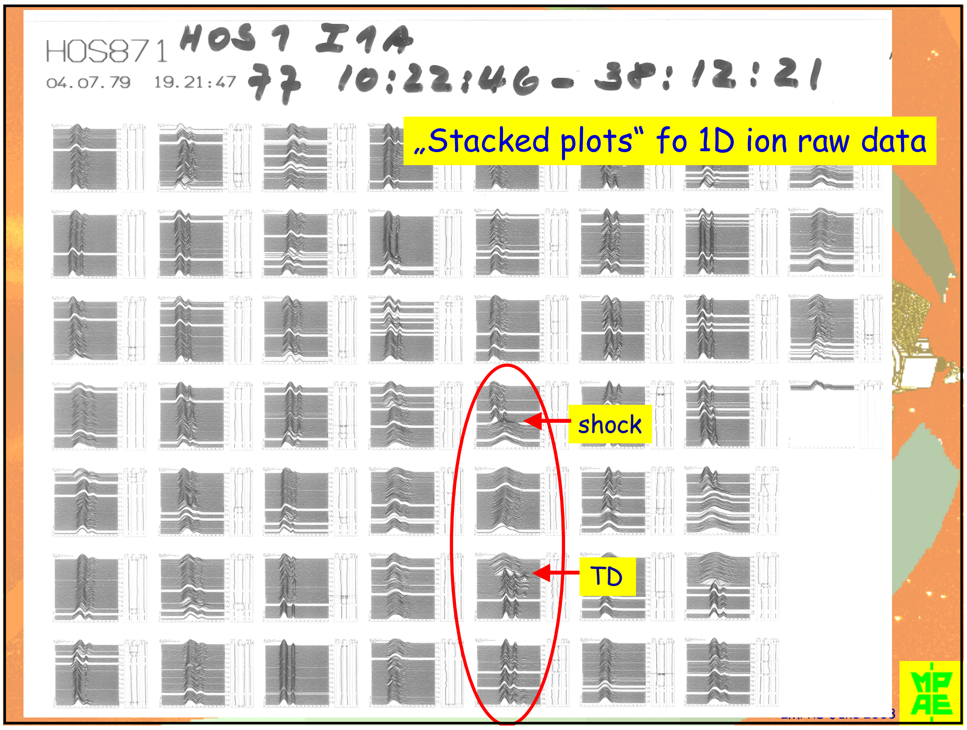
HOS871
04.07.79 19.21:47
„Stacked plots" fo 1D ion raw data
shock
TD

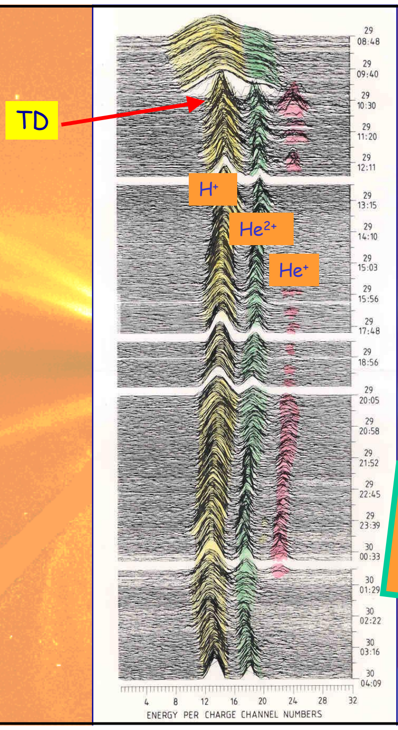

Discovery of singly ionized Helium ions in the driver gas following an interplanetary shock wave by **Helios 1** in January 1977: remnants of cold prominence material.

This discovery was only possible when we began routine inspection of E/Q spectra, i.e. raw data!

There was only one more such event in July 1977. The next one occurred not earlier than in January 1997, following the halo event on Jan. 6th.

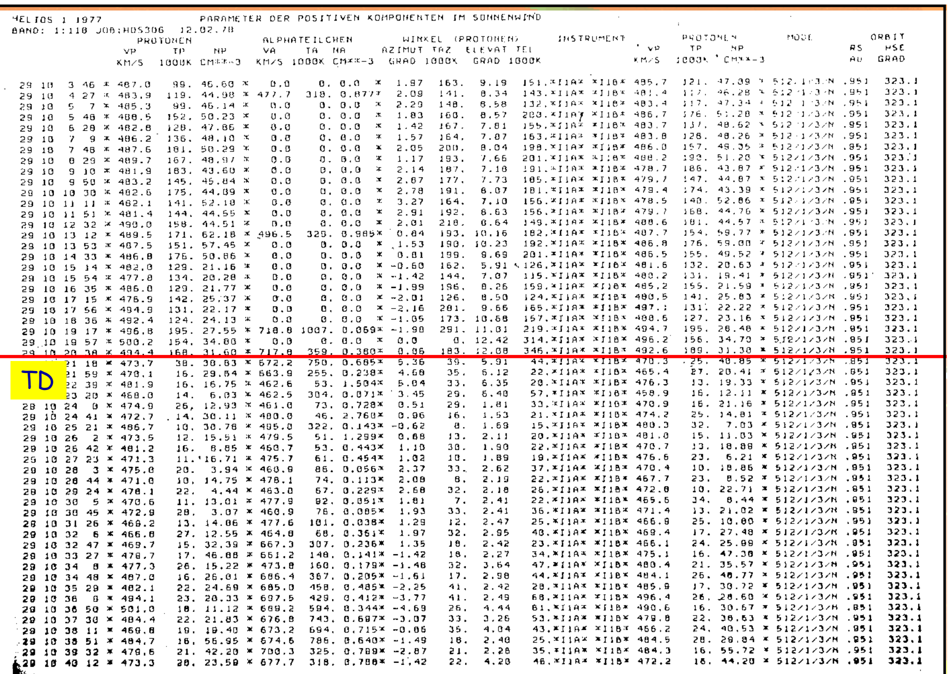

HELIOS 1 1977 PARAMETER DER POSITIVEN KOMPONENTEN IM SONNENWIND

BAND: 1:118 JOB:HDS306 12.02.78

				PROTONEN VP KM/S	TP 1000K	NP CM**-3	ALPHATEILCHEN VA KM/S	TA 1000K	NA CM**-3	WINKEL (PROTONEN) AZIMUT GRAD	TAZ 1000K	ELEVAT GRAD	TEL 1000K	INSTRUMENT	PROTONEN VP KM/S	TP 1000K	NP CM**-3	MODE	ORBIT RS AU	HSE GRAD
29	10	3	46	487.0	99.	46.60	0.0	0.	0.0	1.87	163.	9.19	151.	*I1A* *I1B*	485.7	121.	47.09	512/1/3/N	.951	323.1
29	10	4	27	483.9	119.	44.98	477.7	318.	0.877	2.09	141.	8.34	143.	*I1A* *I1B*	481.4	117.	46.28	512/1/3/N	.951	323.1
29	10	5	7	485.3	99.	46.14	0.0	0.	0.0	2.29	148.	8.58	132.	*I1A* *I1B*	483.4	117.	47.34	512/1/3/N	.951	323.1
29	10	5	48	488.5	152.	50.23	0.0	0.	0.0	1.83	160.	8.57	203.	*I1A* *I1B*	486.7	176.	51.28	512/1/3/N	.951	323.1
29	10	6	28	482.8	128.	47.86	0.0	0.	0.0	1.42	167.	7.81	155.	*I1A* *I1B*	483.7	137.	48.62	512/1/3/N	.951	323.1
29	10	7	9	486.2	136.	48.10	0.0	0.	0.0	1.57	164.	7.87	163.	*I1A* *I1B*	483.8	128.	48.26	512/1/3/N	.951	323.1
29	10	7	48	487.6	181.	50.29	0.0	0.	0.0	2.05	200.	8.04	198.	*I1A* *I1B*	486.0	157.	49.35	512/1/3/N	.951	323.1
29	10	8	29	489.7	167.	48.97	0.0	0.	0.0	1.17	193.	7.66	201.	*I1A* *I1B*	488.2	193.	51.20	512/1/3/N	.951	323.1
29	10	9	10	481.9	183.	43.60	0.0	0.	0.0	2.14	187.	7.18	191.	*I1A* *I1B*	478.7	186.	43.87	512/1/3/N	.951	323.1
29	10	9	50	483.2	145.	45.84	0.0	0.	0.0	2.87	177.	7.73	185.	*I1A* *I1B*	479.7	147.	44.87	512/1/3/N	.951	323.1
29	10	10	30	482.6	175.	44.09	0.0	0.	0.0	2.78	191.	8.07	181.	*I1A* *I1B*	479.4	174.	43.39	512/1/3/N	.951	323.1
29	10	11	11	482.1	141.	52.18	0.0	0.	0.0	3.27	164.	7.10	156.	*I1A* *I1B*	478.5	140.	52.86	512/1/3/N	.951	323.1
29	10	11	51	481.4	144.	44.55	0.0	0.	0.0	2.91	192.	8.63	156.	*I1A* *I1B*	479.7	168.	44.76	512/1/3/N	.951	323.1
29	10	12	32	490.0	158.	44.51	0.0	0.	0.0	2.01	218.	8.64	149.	*I1A* *I1B*	488.6	181.	44.57	512/1/3/N	.951	323.1
29	10	13	12	489.5	171.	62.18	496.5	329.	0.985	0.84	193.	10.16	182.	*I1A* *I1B*	487.7	154.	59.77	512/1/3/N	.951	323.1
29	10	13	53	487.5	151.	57.45	0.0	0.	0.0	1.53	190.	10.23	192.	*I1A* *I1B*	486.8	176.	59.00	512/1/3/N	.951	323.1
29	10	14	33	486.8	176.	50.86	0.0	0.	0.0	0.81	199.	9.69	201.	*I1A* *I1B*	486.5	155.	49.52	512/1/3/N	.951	323.1
29	10	15	14	482.0	129.	21.16	0.0	0.	0.0	-0.60	162.	5.91	126.	*I1A* *I1B*	481.6	132.	20.63	512/1/3/N	.951	323.1
29	10	15	54	477.8	134.	20.28	0.0	0.	0.0	-1.42	144.	7.07	115.	*I1A* *I1B*	480.2	131.	19.41	512/1/3/N	.951	323.1
29	10	16	35	486.0	129.	21.77	0.0	0.	0.0	-1.99	196.	8.26	159.	*I1A* *I1B*	485.2	155.	21.59	512/1/3/N	.951	323.1
29	10	17	15	476.9	142.	25.37	0.0	0.	0.0	-2.01	126.	8.50	124.	*I1A* *I1B*	480.5	141.	25.83	512/1/3/N	.951	323.1
29	10	17	56	494.9	131.	22.17	0.0	0.	0.0	-2.16	201.	9.66	165.	*I1A* *I1B*	497.1	131.	22.22	512/1/3/N	.951	323.1
29	10	18	36	492.4	124.	24.13	0.0	0.	0.0	-1.05	173.	10.68	157.	*I1A* *I1B*	488.6	127.	23.16	512/1/3/N	.951	323.1
29	10	19	17	496.8	195.	27.55	718.8	1007.	0.069	-1.98	291.	11.01	219.	*I1A* *I1B*	494.7	195.	28.48	512/1/3/N	.951	323.1
29	10	19	57	500.2	154.	34.88	0.0	0.	0.0	0.0	0.	12.42	314.	*I1A* *I1B*	496.2	156.	34.70	512/1/3/N	.951	323.1
29	10	20	38	494.4	168.	31.60	717.8	359.	0.380	0.06	183.	12.08	346.	*I1A* *I1B*	492.6	189.	31.30	512/1/3/N	.951	323.1
[illegible]	[illegible]	21	18	473.7	38.	38.83	672.2	750.	0.685	5.36	39.	5.91	44.	*I1A* *I1B*	470.3	25.	40.85	512/1/3/N	.951	323.1
[illegible]	[illegible]	21	59	470.1	16.	29.64	663.9	255.	0.238	4.68	35.	6.12	22.	*I1A* *I1B*	465.4	27.	20.41	512/1/3/N	.951	323.1
[illegible]	[illegible]	22	39	481.9	16.	16.75	462.6	53.	1.504	5.04	33.	6.35	20.	*I1A* *I1B*	476.3	13.	19.33	512/1/3/N	.951	323.1
[illegible]	[illegible]	23	20	460.0	14.	6.03	462.5	304.	0.071	3.45	29.	6.40	57.	*I1A* *I1B*	458.9	16.	12.11	512/1/3/N	.951	323.1
29	10	24	0	474.9	26.	12.93	461.0	73.	0.728	0.51	29.	1.81	33.	*I1A* *I1B*	470.9	16.	21.16	512/1/3/N	.951	323.1
29	10	24	41	472.7	14.	30.11	480.0	46.	2.760	0.96	16.	1.53	21.	*I1A* *I1B*	474.2	25.	14.81	512/1/3/N	.951	323.1
29	10	25	21	486.7	10.	30.78	485.0	322.	0.143	-0.62	8.	1.69	15.	*I1A* *I1B*	480.3	32.	7.03	512/1/3/N	.951	323.1
29	10	26	2	473.5	12.	15.51	479.5	51.	1.299	0.68	13.	2.11	20.	*I1A* *I1B*	481.0	15.	11.03	512/1/3/N	.951	323.1
29	10	26	42	481.2	16.	8.85	460.7	53.	0.443	1.10	30.	1.90	22.	*I1A* *I1B*	470.7	13.	18.88	512/1/3/N	.951	323.1
29	10	27	23	471.3	11.	16.71	475.7	61.	0.454	1.02	10.	1.89	19.	*I1A* *I1B*	476.6	23.	6.21	512/1/3/N	.951	323.1
29	10	28	3	475.0	20.	3.94	460.9	86.	0.056	2.37	33.	2.62	37.	*I1A* *I1B*	470.4	10.	18.86	512/1/3/N	.951	323.1
29	10	28	44	471.0	10.	14.75	478.1	74.	0.113	2.08	8.	2.19	22.	*I1A* *I1B*	467.7	23.	8.52	512/1/3/N	.951	323.1
29	10	29	24	478.1	22.	4.44	463.0	67.	0.229	2.68	32.	2.18	26.	*I1A* *I1B*	472.8	10.	22.71	512/1/3/N	.951	323.1
29	10	30	5	470.6	11.	13.01	477.9	92.	0.051	1.81	7.	2.41	22.	*I1A* *I1B*	465.6	34.	8.44	512/1/3/N	.951	323.1
29	10	30	45	472.9	28.	3.07	460.9	76.	0.085	1.93	33.	2.41	36.	*I1A* *I1B*	471.4	13.	21.02	512/1/3/N	.951	323.1
29	10	31	26	468.2	13.	14.06	477.6	101.	0.038	1.29	12.	2.47	25.	*I1A* *I1B*	466.8	25.	10.00	512/1/3/N	.951	323.1
29	10	32	6	466.8	27.	12.55	464.8	68.	0.361	1.97	32.	2.95	40.	*I1A* *I1B*	469.4	17.	27.48	512/1/3/N	.951	323.1
29	10	32	47	469.7	15.	32.39	667.3	307.	0.236	1.35	18.	2.42	23.	*I1A* *I1B*	466.1	24.	25.88	512/1/3/N	.951	323.1
29	10	33	27	478.7	17.	46.88	661.2	140.	0.141	-1.42	18.	2.27	34.	*I1A* *I1B*	475.1	16.	47.30	512/1/3/N	.951	323.1
29	10	34	8	477.3	26.	15.22	473.8	160.	0.179	-1.46	32.	3.64	47.	*I1A* *I1B*	480.4	21.	35.57	512/1/3/N	.951	323.1
29	10	34	48	487.0	16.	26.01	686.4	367.	0.205	-1.61	17.	2.98	44.	*I1A* *I1B*	484.1	26.	40.77	512/1/3/N	.951	323.1
29	10	35	29	482.1	22.	24.69	685.0	458.	0.485	-2.25	41.	2.42	28.	*I1A* *I1B*	485.9	17.	30.72	512/1/3/N	.951	323.1
29	10	36	8	494.1	23.	20.33	697.5	429.	0.412	-3.77	41.	2.49	68.	*I1A* *I1B*	496.4	26.	28.60	512/1/3/N	.951	323.1
29	10	36	50	501.0	18.	11.12	689.2	594.	0.344	-4.69	26.	4.44	61.	*I1A* *I1B*	490.6	16.	30.67	512/1/3/N	.951	323.1
29	10	37	30	484.4	22.	21.83	676.8	743.	0.697	-3.07	33.	3.26	53.	*I1A* *I1B*	479.8	22.	38.63	512/1/3/N	.951	323.1
29	10	38	11	469.8	19.	19.40	673.2	694.	0.715	-0.06	35.	4.04	43.	*I1A* *I1B*	466.2	24.	40.53	512/1/3/N	.951	323.1
29	10	38	51	484.7	16.	56.95	674.6	786.	0.640	-1.49	18.	2.40	25.	*I1A* *I1B*	484.5	28.	28.84	512/1/3/N	.951	323.1
29	10	39	32	478.6	21.	42.20	700.3	325.	0.789	-2.87	21.	2.28	35.	*I1A* *I1B*	484.3	16.	55.72	512/1/3/N	.951	323.1
29	10	40	12	473.3	28.	23.59	677.7	318.	0.788	-1.42	22.	4.20	46.	*I1A* *I1B*	472.2	16.	44.20	512/1/3/N	.951	323.1

Solar wind ion parameter data from Helios E1-I1a/I1b

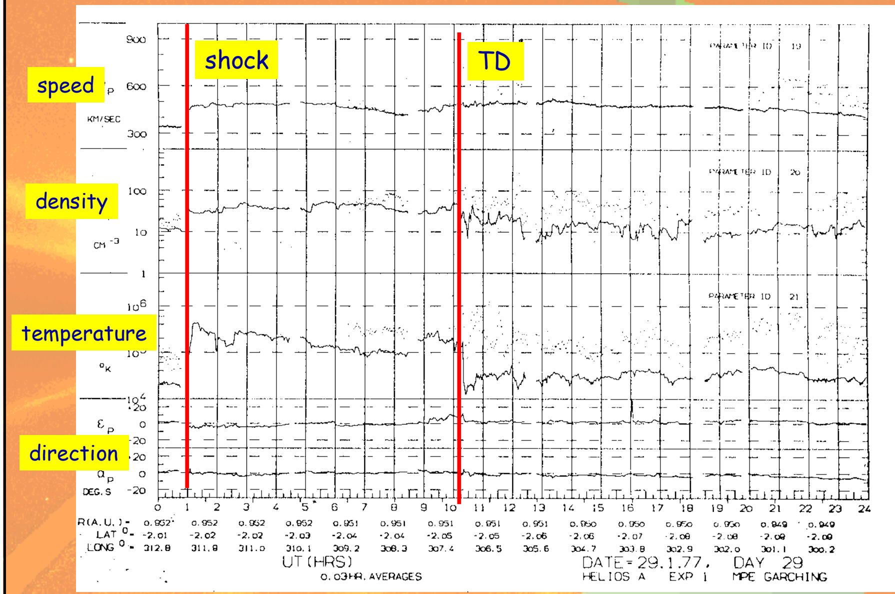

24 hrs routine plot of Helios E1 ion data (3 min averages)

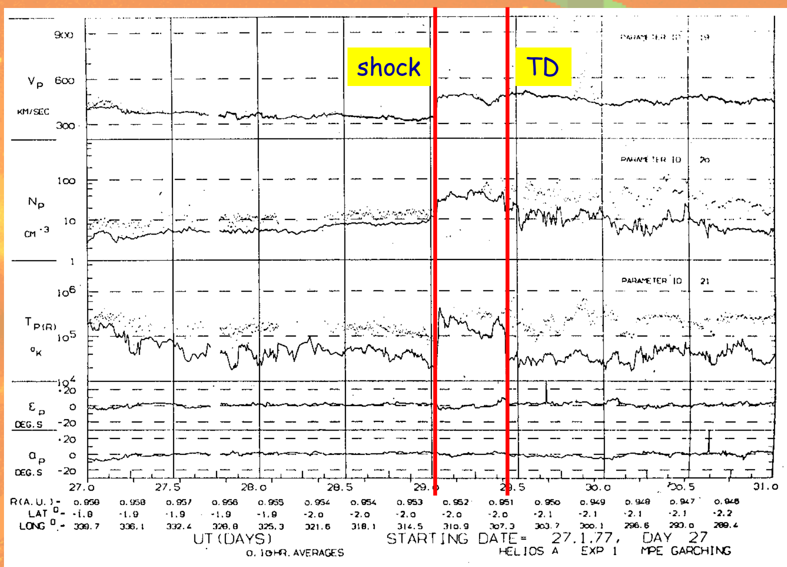

4 days routine plot of Helios E1 ion data (10 min averages)

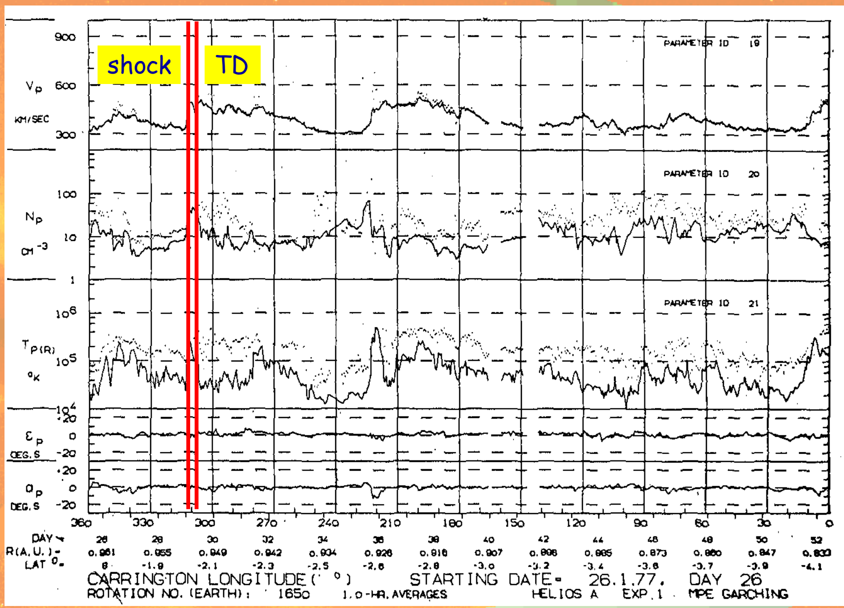

Carrington routine plot of Helios E1 ion data (1 hr averages)

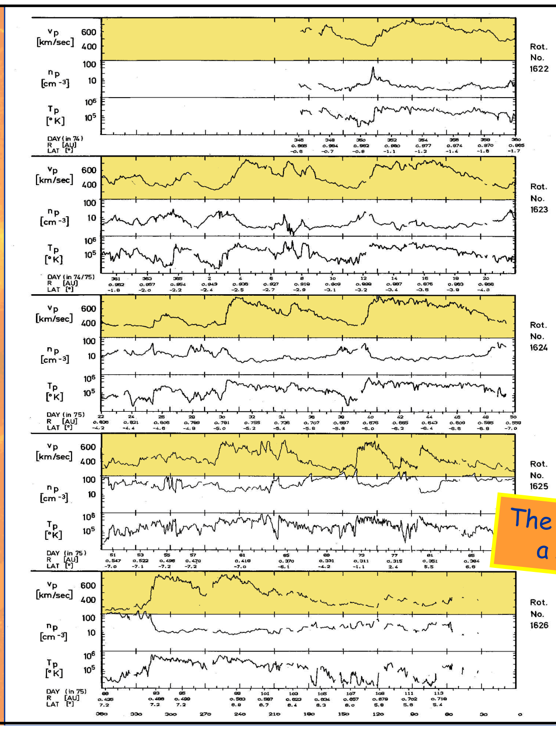

Helios plasma measurements during first approach to perihelion (0.3 AU).

The stream fronts become steeper, a surprise for some modelers...

Since 1974, all these various data collections were stored on tapes and printed on paper and microfiches. A major problem: the data had to be adjusted to at least five subsequent computer generations. Presently, the data are available on CD-Rom and on the Internet

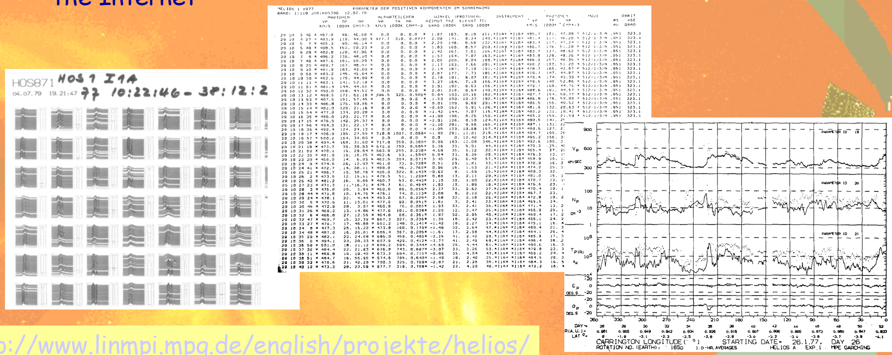

http://www.linmpi.mpg.de/english/projekte/helios/

http://sprg.ssl.berkeley.edu/htbin/impact/HeliosData.pl

http://sec.noaa.gov/ace/

http://umtof.umd.edu/pm

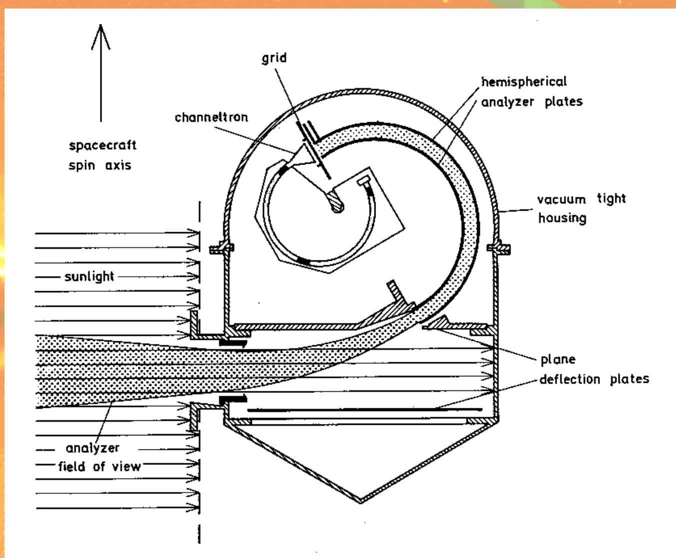

Scheme of the Helios E1 electron instrument (I2), invented by H. Rosenbauer.
The trick: no photo electron could ever make it to the detector!

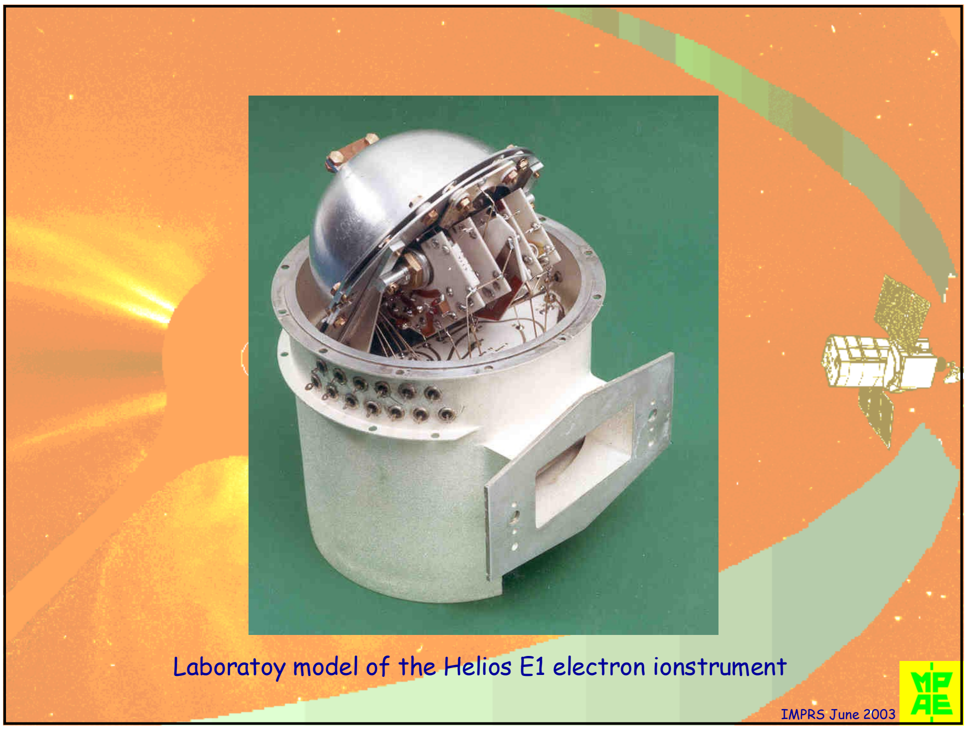
Laboratoy model of the Helios E1 electron ionstrument
IMPRS June 2003

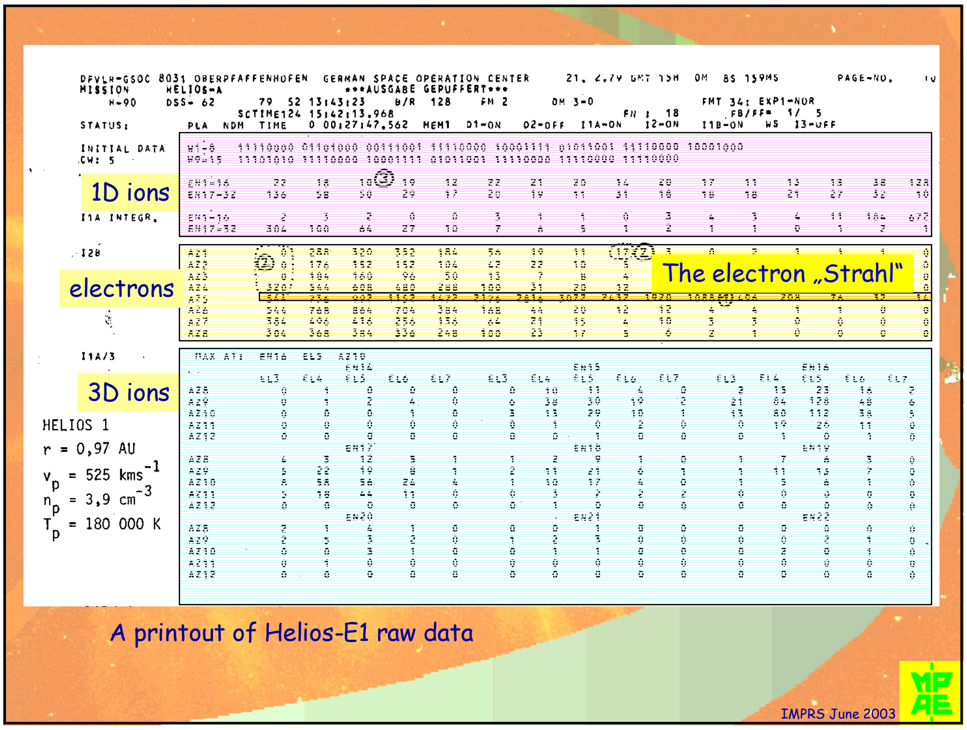
1D ions
electrons
The electron „Strahl"
3D ions
HELIOS 1
r = 0,97 AU
v_p = 525 kms^{-1}
n_p = 3,9 cm^{-3}
T_p = 180 000 K
A printout of Helios-E1 raw data
IMPRS June 2003

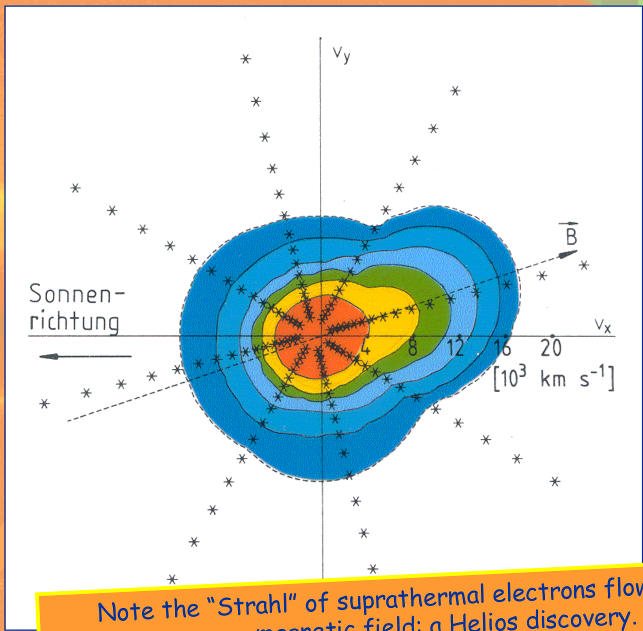

Electron velocity distributions as measured by Helios E1-I2

Note the "Strahl" of suprathermal electrons flowing along the magnetic field: a Helios discovery.

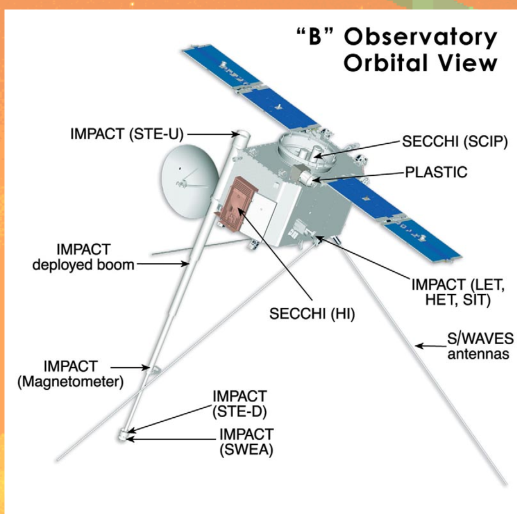

STEREO spacecraft: Note the electron instrument (SWEA) on the end of the backside boom. It has a field of view of nearly 4π, and it is located in permanent shadow.

http://projects.nrl.navy.mil/secchi/spacecraft.html

The problem of electrostatic analyzers

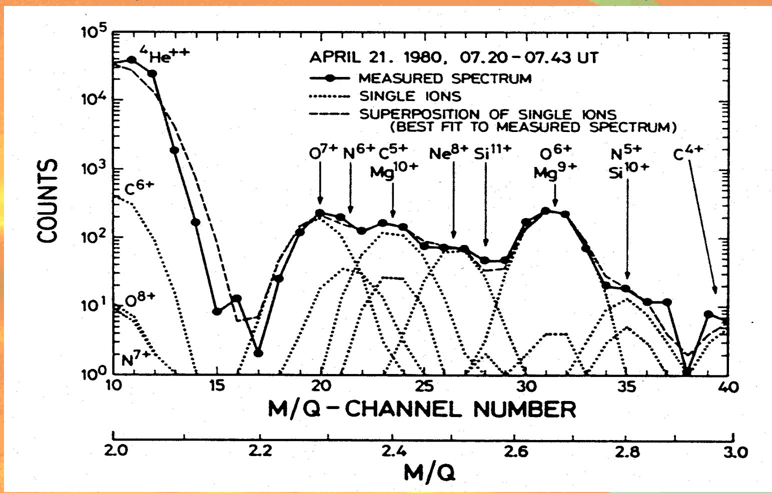

The E/q value is not unique: $E/q = \frac{1}{2}\, m v^2/nq_0$.
Fortunately, in the solar wind all ions come with about the same velocity v_{sw}
(apart from their individual thermal speeds).

Therefore, $E/q \sim m/nq_0$

The problem of electrostatic analyzers

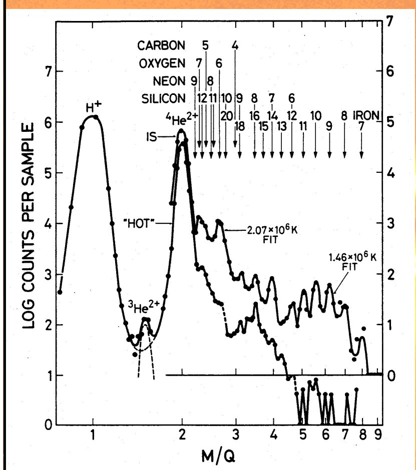

Figure 13: Two E/Q spectra (converted into M/Q) registered by the Los Alamos instrument on Vela 6B showing different freezing-in conditions of the charge states of the elements (Bame, 1983). The upper spectrum represents typical interstream stream (IS) charge state distributions. The lower, "hot" spectrum is characterized by much higher degrees of ionization. The peak at M/Q = 3.5 represents the particularly stable Fe^{16+} ion. The abundance of O^{6+} is very low, presumably most of the oxygen is in the O^{8+} state which is hidden by $^{4}He^{2+}$. The number of ions that can be identified under such "hot" conditions in E/Q or M/Q spectra is small, because the ionic states of most of the abundant elements are compressed towards M/Q = 2 (cf. Figure 15).

The m/q values of many fully ionized ions are identical,
e.g. $^{4}He^{2+}$, $^{12}C^{6+}$, $^{14}N^{7+}$, $^{16}O^{8+}$,...

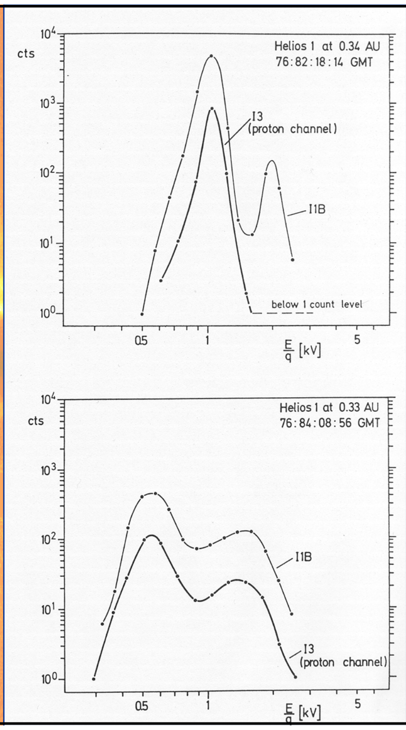

The second peak in an E/q spectrum is usually due to Helium ions. That's why they were clearly discarded when I3 was working in the proton channel.

Instrument I3 of **Helios-E1** was the first solar wind ion mass spectrometer. It measured E/q and, independently v. It could not overcome the m/q problem.

In this case, however, the second peak was due to protons, i.e., a second proton population moving at a different speed!

IMPRS June 2003

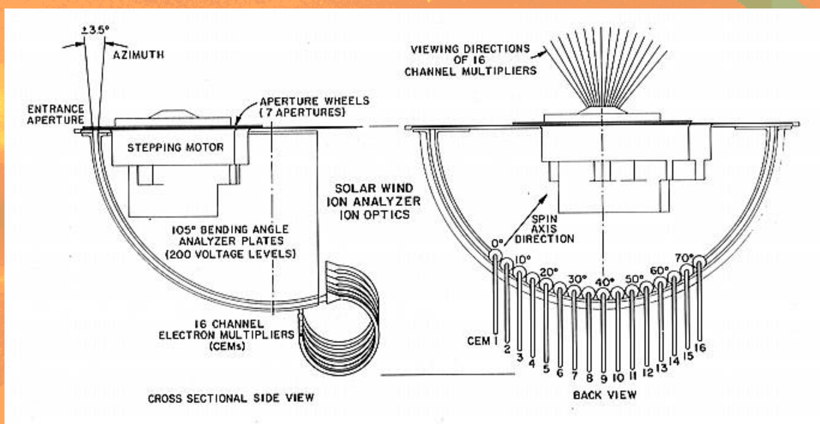

The SWOOPS ion instrument on Ulysses, built by LANL

http://swoops.lanl.gov/

IMPRS June 2003

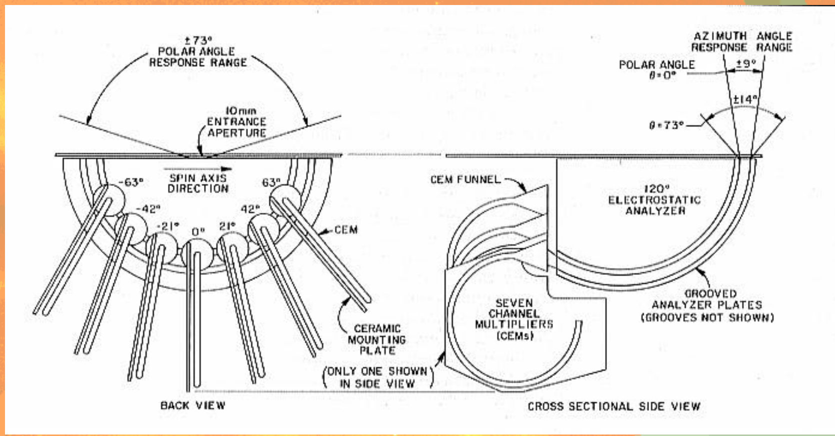

The SWOOPS electron instrument on Ulysses, built by LANL

http://swoops.lanl.gov/

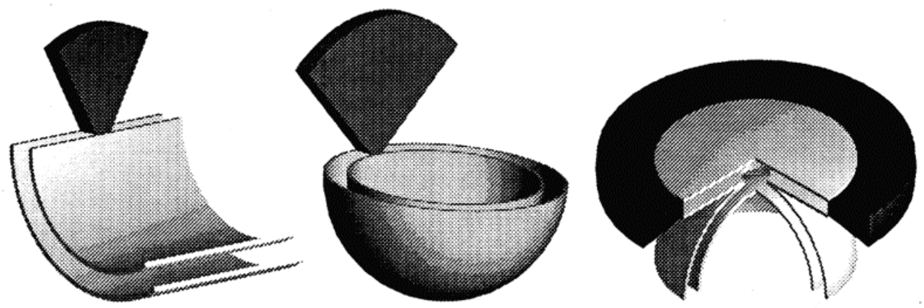

Fig. 1. Evolution of the electrostatic analyzer used in space plasma diagnostics: (a) cylindrical analyzer, (b) spherical analyzer, and (c) top-hat analyzer. The dark regions illustrate the field of view.

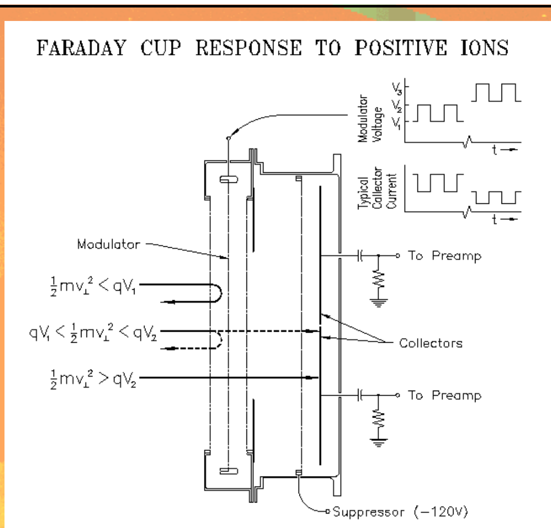

An alternative to electrostatic analyzers: the Farady cup. It achieves E/q resolution by varying the voltages on the various grids. This technique was used mainly by the MIT group, e.g., on the Voyager space probes.

http://voyager.jpl.nasa.gov/

Electrostatic analyzer complemented with a magnetic deflection system

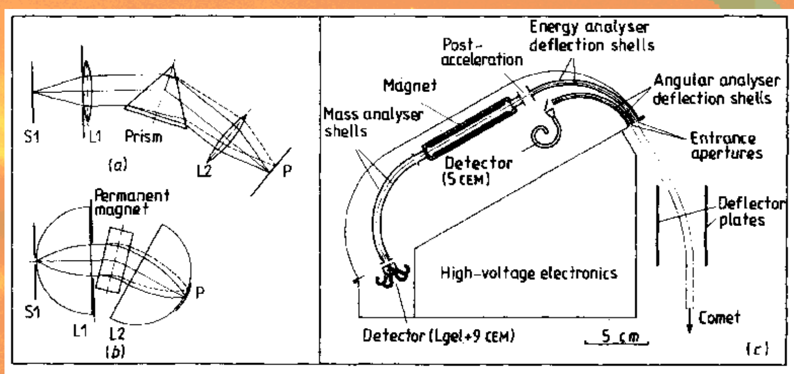

The ions with identical E/q enter a homogeneous magnetic field. There, they are deflected according to their different momenta, i.e. mv/q values. They are then collected in separate detectors. This detector works best if v is identical for all ions, e.g. during the approach to comet Halley (70 km/s)

The Giotto-IMS HIS*, invented by H. Rosenbauer

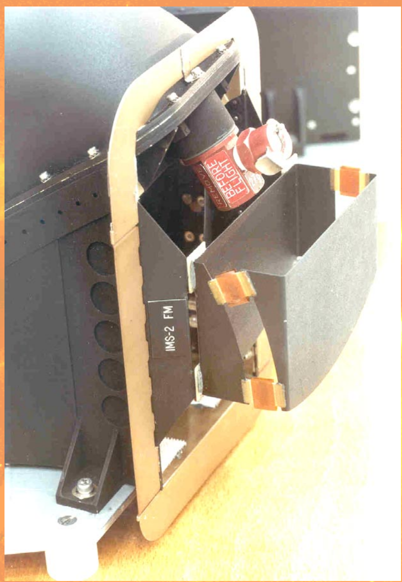

The entrance deflector of the HIS flight unit

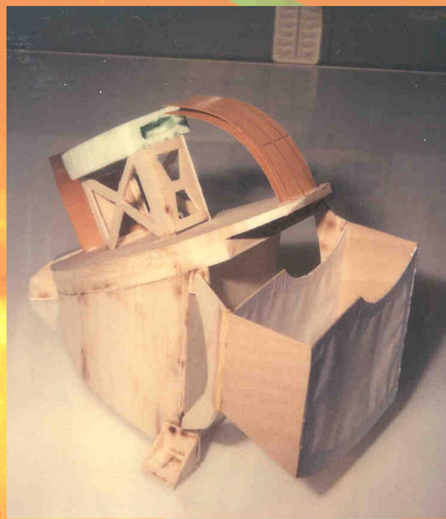

An early 3D study model, plywood...

* HIS: High Intensity Spectrometer

IMPRS June 2003

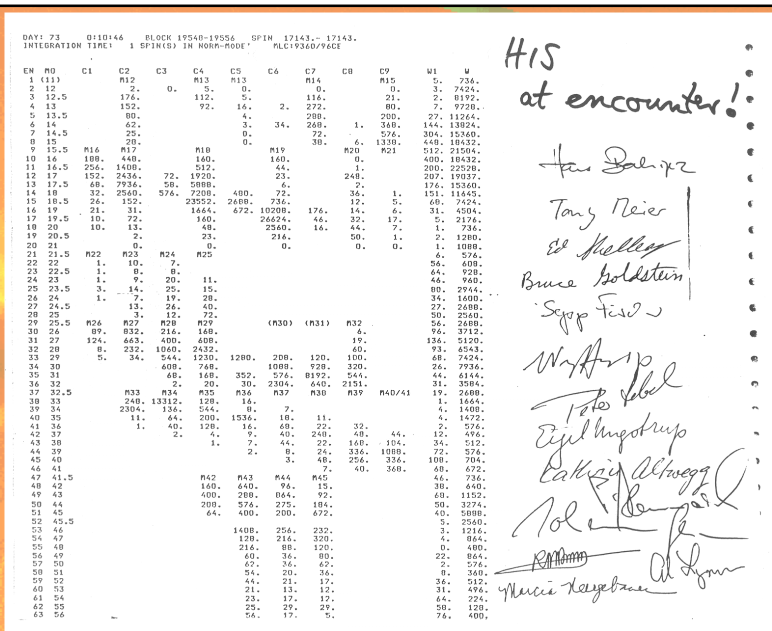

DAY: 73 0:10:46 BLOCK 19548-19556 SPIN 17143.- 17143.
INTEGRATION TIME: 1 SPIN(S) IN NORM-MODE' MLC:9360/96CE

EN	MO	C1	C2	C3	C4	C5	C6	C7	C8	C9	W1	W
1	(11)		M12		M13	M13		M14		M15	5.	736.
2	12		2.	0.	5.	0.		0.		0.	3.	7424.
3	12.5		176.		112.	5.		116.		21.	2.	8192.
4	13		152.		92.	16.	2.	272.		80.	7.	9728.
5	13.5		80.			4.		288.		200.	27.	11264.
6	14		62.			3.	34.	268.	1.	368.	144.	13824.
7	14.5		25.			0.		72.		576.	304.	15360.
8	15		28.			0.		38.	6.	1338.	448.	18432.
9	15.5	M16	M17		M18		M19		M20	M21	512.	21504.
10	16	188.	448.		160.		160.		0.		400.	18432.
11	16.5	256.	1408.		512.		44.		1.		200.	22528.
12	17	152.	2436.	72.	1920.		23.		248.		207.	19037.
13	17.5	68.	7936.	58.	5888.		6.		2.		176.	15360.
14	18	32.	2560.	576.	7208.	480.	72.		36.	1.	151.	11645.
15	18.5	26.	152.		23552.	2688.	736.		12.	5.	68.	7424.
16	19	21.	31.		1664.	672.	10208.	176.	14.	6.	31.	4504.
17	19.5	10.	72.		160.		26624.	46.	32.	17.	5.	2176.
18	20	10.	13.		48.		2560.	16.	44.	7.	1.	736.
19	20.5		2.		23.		216.		50.	1.	2.	1280.
20	21		0.		0.		0.		0.	0.	1.	1088.
21	21.5	M22	M23	M24	M25						6.	576.
22	22	1.	10.	7.							56.	608.
23	22.5	1.	8.	8.							64.	928.
24	23	1.	9.	20.	11.						46.	960.
25	23.5	3.	14.	25.	15.						80.	2944.
26	24	1.	7.	19.	28.						34.	1600.
27	24.5		13.	26.	40.						27.	2688.
28	25		3.	12.	72.						50.	2560.
29	25.5	M26	M27	M28	M29		(M30)	(M31)	M32		56.	2688.
30	26	89.	832.	216.	168.				6.		96.	3712.
31	27	124.	663.	400.	608.				19.		136.	5120.
32	28	8.	232.	1060.	2432.				60.		93.	6543.
33	29	5.	34.	544.	1230.	1280.	208.	120.	100.		68.	7424.
34	30			608.	768.		1088.	928.	320.		26.	7936.
35	31			68.	168.	352.	576.	8192.	544.		44.	6144.
36	32			2.	20.	30.	2304.	640.	2151.		31.	3584.
37	32.5		M33	M34	M35	M36	M37	M38	M39	M40/41	19.	2688.
38	33		248.	13312.	128.	16.					1.	1664.
39	34		2304.	136.	544.	8.	7.				4.	1408.
40	35		11.	64.	200.	1536.	18.	11.			4.	1472.
41	36		1.	40.	128.	16.	68.	22.	32.		2.	576.
42	37			2.	4.	9.	40.	248.	48.	44.	12.	496.
43	38				1.	7.	44.	22.	168.	104.	34.	512.
44	39					2.	8.	24.	336.	1088.	72.	576.
45	40						3.	48.	256.	336.	108.	704.
46	41							7.	40.	368.	68.	672.
47	41.5				M42	M43	M44	M45			46.	736.
48	42				160.	640.	96.	15.			38.	640.
49	43				400.	288.	864.	92.			68.	1152.
50	44				208.	576.	275.	184.			50.	3274.
51	45				64.	400.	200.	672.			40.	5888.
52	45.5										5.	2560.
53	46					1408.	256.	232.			3.	1216.
54	47					128.	216.	320.			4.	864.
55	48					216.	88.	120.			0.	480.
56	49					60.	36.	80.			22.	864.
57	50					62.	36.	62.			2.	576.
58	51					54.	20.	36.			8.	368.
59	52					44.	21.	17.			36.	512.
60	53					21.	13.	12.			31.	496.
61	54					23.	17.	12.			64.	224.
62	55					25.	29.	29.			58.	128.
63	56					56.	17.	5.			76.	400,

Ion mass spectrum raw data at comet Halley, obtained by the Giotto IMS-HIS instrument

IMPRS June 2003

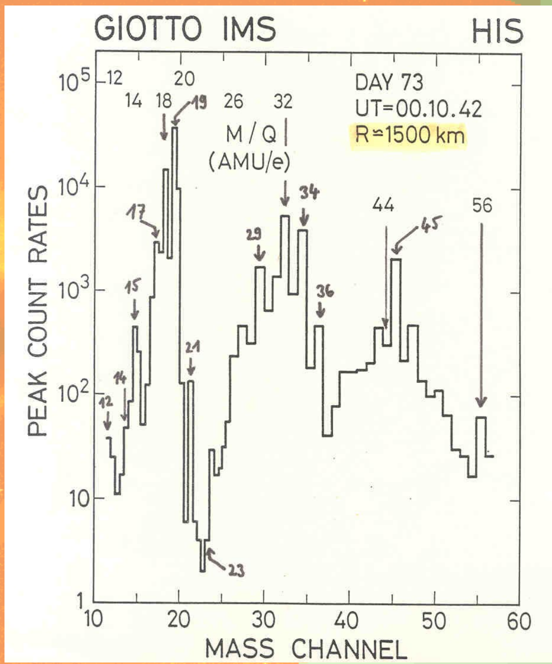

Ion mass spectra obtained inside the coma of comet Halley, by the Giotto IMS-HIS instrument

IMPRS June 2003

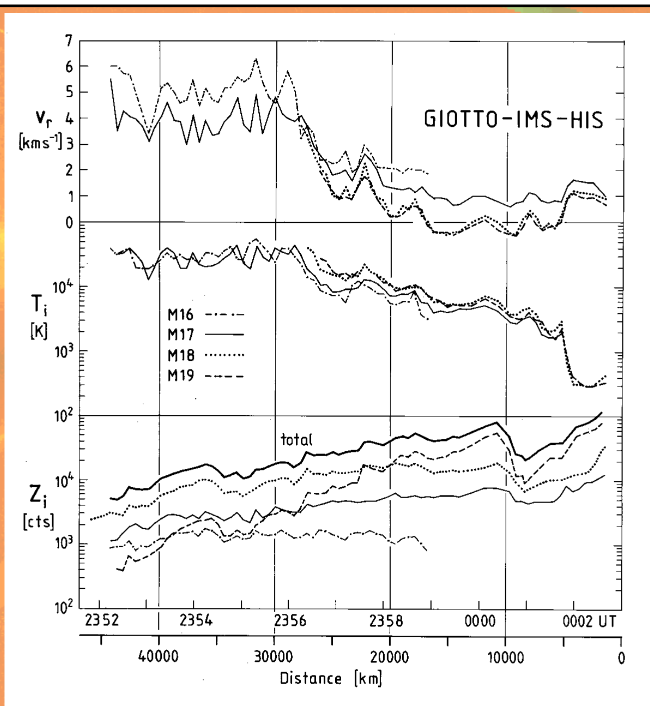

Ion density profiles during the approach to comet Halley, obtained by the Giotto IMS-HIS instrument

IMPRS June 2003

The Giotto-IMS HERS*, invented by M. Neugebauer

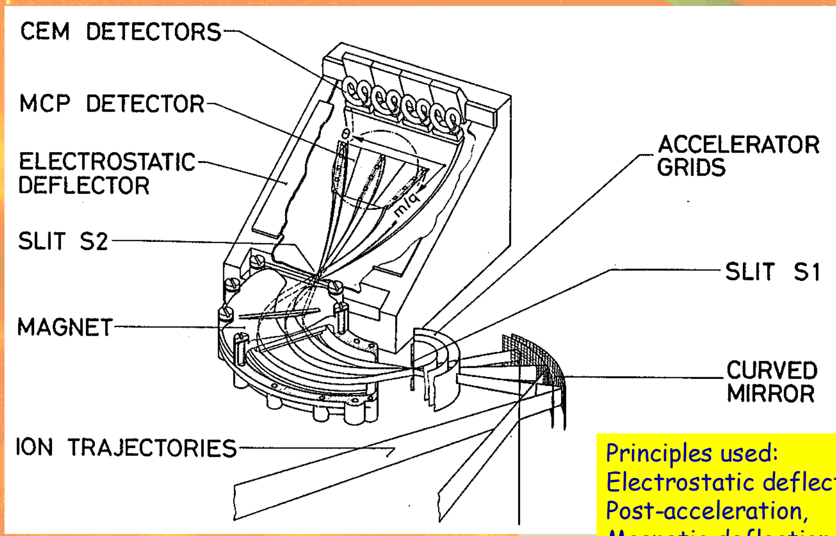

Principles used:
Electrostatic deflection,
Post-acceleration,
Magnetic deflection

* HERS: High Energy Range Spectrometer

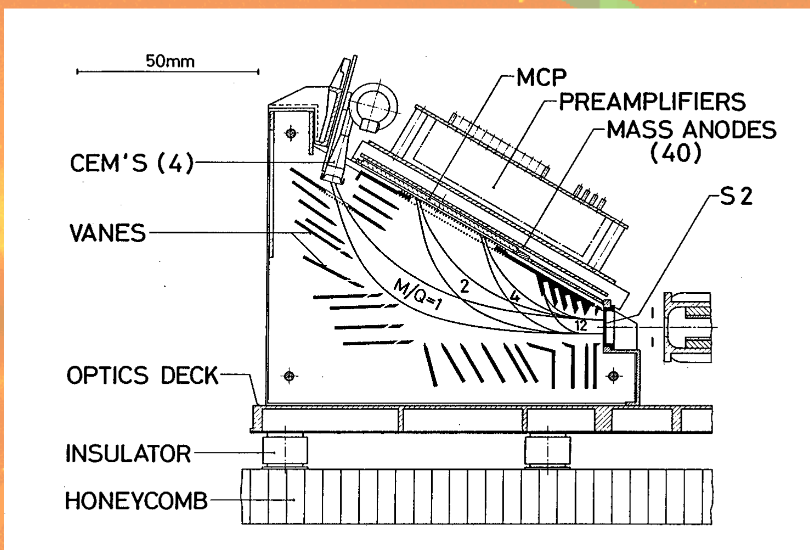

The analyzer section of the HERS instrument

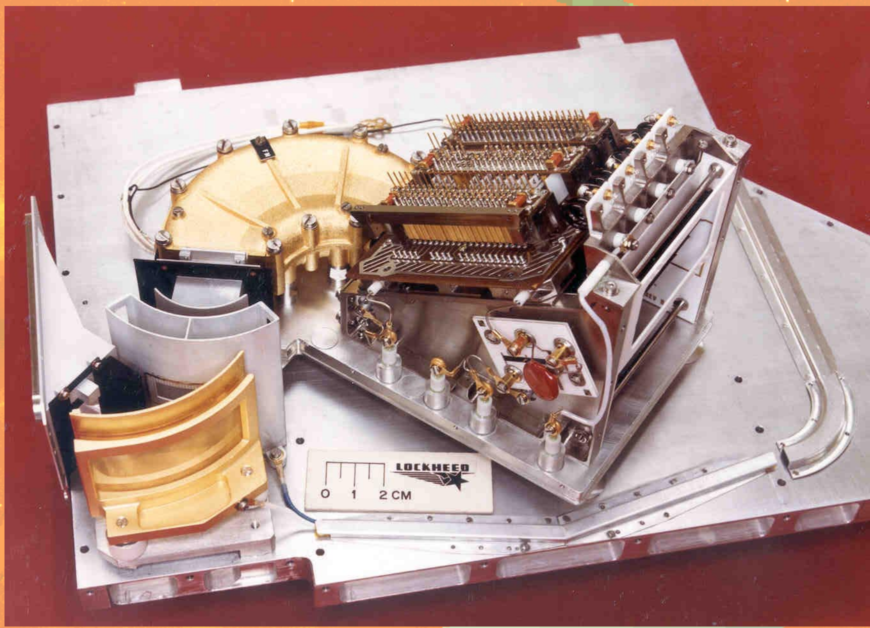

The HERS sensor parts